



# Significant thermal conductivity enhancement for nanofluids containing graphene nanosheets

Wei Yu<sup>a,b</sup>, Huaqing Xie<sup>a,\*</sup>, Xiaoping Wang<sup>a</sup>, Xinwei Wang<sup>b</sup>

<sup>a</sup> School of Urban Development and Environmental Engineering, Shanghai Second Polytechnic University, Shanghai 201209, PR China

<sup>b</sup> Department of Mechanical Engineering, Iowa State University, Ames, IA 50011-2161, USA

## ARTICLE INFO

### Article history:

Received 11 November 2010  
 Received in revised form 17 January 2011  
 Accepted 20 January 2011  
 Available online 22 January 2011  
 Communicated by F. Porcelli

### Keywords:

Graphene  
 Nanofluid  
 Thermal conductivity  
 Heat transfer

## ABSTRACT

We developed a facile technique to produce ethylene glycol based nanofluids containing graphene nanosheets. The thermal conductivity of the base fluid was increased significantly by the dispersed graphene: up to 86% increase for 5.0 vol% graphene dispersion. The 2D structure and stiffness of graphene and graphene oxide help to increase the thermal conductivity of the nanofluid. The thermal conductivity of graphene oxide and graphene in the fluid were estimated to be  $\sim 4.9$  and  $6.8$  W/mK, respectively.

© 2011 Elsevier B.V. All rights reserved.

## 1. Introduction

Graphene is a flat monolayer of  $sp^2$ -bonded carbon atoms tightly packed into a honeycomb lattice. It has attracted much attention due to the two-dimensional structure, exceptional physical and chemical properties [1]. Graphene has exhibited some unusual electrical, mechanical and thermal behaviors, such as very high carrier mobility [2], long-range ballistic transport at room temperature [3], quantum confinement in nanoscale ribbons [4], and single-molecule gas detection sensitivity [5]. Therefore, graphene has various potential applications [6].

Balandin et al. discovered that graphene exhibited far better thermal conductivity than carbon nanotubes [7]. Their results opened a new window to graphene applications in heat management of high-power electronics. It is an important discovery, and then in the following years theoretical and experimental investigations about the heat transfer properties of graphene have become one of the hot topics of physics. Balandin et al. proposed a model for the lattice thermal conductivity of graphene in the framework of Klemens approximation [8]. The phonon mean free path was about 775 nm near room temperature [9]. They calculated the phonon thermal conductivity of single-layer graphene at room-temperature to be in the range of 2000–5000 W/mK depending on the flake width, defect concentration and roughness of the edges [10,11]. The nonequilibrium molecular dynamics method was used

to investigate thermal conductivity of graphene nanoribbons with different edge shapes, and the results indicated the strong length dependence of thermal conductivity [12]. The evident thermal rectification for asymmetric nanoribbons was found [13]. Striolo et al. applied molecular dynamics simulations to investigate the thermal boundary resistance at the graphene–oil interface [14]. They found that the Kapitza resistance at the graphene sheet–liquid octane interface was reduced by appropriately functionalizing the graphene sheet. The heat transfer study of graphite nanoplatelet–epoxy composites showed that few graphene layer was an efficient filler for the thermal conductivity enhancement of epoxy composites [15]. Some recent theoretical work shows that the interfacial resistances to heat transfer (Kapitza resistances) are responsible for the lower-than-expected thermal conductivity of nanocomposites [16,17], and much work should be done to reduce the Kapitza resistances.

In contrast to the theoretical study of the thermal conductivity of graphene, the experimental work about the heat transfer property of graphene-based materials is rare. One of the important factors restricting the implication of graphene is that graphene is incompatible with the matrix. The excellent performance of nanocomposites depends not only on the intrinsic properties of the nanofiller, but also on the compatibility between nanofiller and matrix. Up to date, chemical methods for the production of graphene are scalable [18], while the reduction of exfoliated graphene oxide nanoplates in water results in their irreversible coagulation, which makes dispersion within a matrix at the individual sheet level impossible [19]. The direct dispersion of hydrophobic graphite or graphene sheets in polar solvents without

\* Corresponding author. Tel. & fax: +86 21 50217331.  
 E-mail address: hqxie@eed.spu.cn (H. Xie).

the assistance of dispersing agents has generally been considered to be a great challenge [20]. One of the important parts in the work is to enhance the compatibility between graphene and the matrix.

In the past decade, nanofluids have attracted much attention due to their considerable increase in thermal conductivity compared with the base fluids [21,22]. In our previous work [23], we investigated the heat transfer property of ethylene glycol (EG) based nanofluids containing graphene oxide nanosheets (GON), and the results demonstrated that graphene oxide was a good additive to enhance the thermal conductivity of the base fluid. It is no doubt that graphene will have higher thermal conductivity than graphene oxide, therefore it will be very interesting to study the thermal transport properties of graphene-based nanofluids, and to explore how much it improves in thermal conductivity compared with graphene oxide-based nanofluids. In this work, we designed a simple method to prepare hydrophilic graphene, and then we obtained the ethylene glycol nanofluids containing graphene nanosheets (GN-EG nanofluids). The heat transfer properties of the nanofluids were investigated.

## 2. Experimental details

The two-step method was used to prepare the graphene nanofluids. The first step is to prepare hydrophilic graphene, and then the graphene would be dispersed in ethylene glycol. First, graphite oxide was obtained through a modified Hummer's method as described elsewhere [24]. Then graphite oxide could be readily exfoliated as individual graphene oxide sheets by ultrasonication in ethanol solution. Graphene oxide was electrically insulating, and it could be converted back to conducting graphene by chemical reduction. Unfortunately, the chemically converted graphene sheets obtained through chemical reduction precipitated as irreversible agglomerates owing to their hydrophobic nature. The graphene agglomerate prepared by the usual method is very hard, even its volume is much smaller than its parent material graphite. The resulting graphene agglomerate is not soluble or redispersible in water or other polar solvents, making further processing difficult. We found that a small change in synthetic process could greatly enhance the dispersion of graphene. Before reduced by hydrazine, the graphene oxide ethanol solution was mixed with the dispersant sodium dodecylbenzenesulfonate (SDBS). During the hydrazine reduction of graphene oxide sheets, the brown-colored dispersion turned black. Then the reduced mixture was washing five times by ethanol to remove the dispersant. The obtained dry graphene was loose black powder like ashes, would fly in the air. Its size was much larger than graphite with the same weight. The obtained graphene could be easily redispersed in polar solvent with a short sonication of less than 5 min. The graphene nanofluids was prepared by the following method: the fixed quality of graphene with different volume fractions ( $\phi$ : 0.01–0.05,  $\phi$  is the volume fraction of GNs) was dispersed in EG. The volume fraction of the powder was calculated from the weight of dry powder using the density of graphite ( $2.62 \text{ g/cm}^3$ ) and the total volume of the suspension. The mass fractions for  $\phi = 0.01, 0.02, 0.03, 0.04$  and  $0.05$  are 2.32, 4.58, 6.79, 8.93 and 11.03 wt%, respectively. The nanofluid mixture was stirred and sonicated using ultrasonic washing machine. Graphene oxide ethanol solution is brown, while the graphene solution is black.

The size and morphology of graphene nanosheets were examined by using transmission electron microscopy (TEM, JEOL 2100F). The TEM samples were prepared by dispersing the powder products in alcohol by ultrasonic treatment, dropping the suspension onto a holey carbon film supported on a copper grid, and drying it in air. AFM images were taken on a MultiTask AutoProbe CP/MT Scanning Probe Microscope (Veeco Instruments, Woodbury, NY).

Imaging was done in tapping mode using a V-shape 'Ultralever' probe B and nominal tip radius 10 nm (Park Scientific Instruments, Woodbury, NY). The diluted graphene alcohol solution was dropped onto the freshly cleaved mica. After the mica was dry, the graphene was imaged. Fourier transform infrared (FT-IR) spectra were obtained using Bruker vertex 70 with KBr method. A thermogravimetric analyzer (TG-DTG, Netzsch STA 449C) was used for thermogravimetric analysis (sample mass: about 15.0 mg; atmosphere, flowing dry nitrogen). A transient short hot-wire (SHW) technique was applied to measure the thermal conductivities of the nanofluids in the temperature range of 10 to  $60^\circ\text{C}$  [25]. In addition to hot-wire system, a temperature-controlled bath was used to maintain different temperatures of nanofluids during the measurement process. The experimental apparatus was calibrated by measuring the thermal conductivity of deionized water, and the accuracy of these measurements was estimated to be within  $\pm 1\%$ . In the thermal conductivity measurements, the vessel containing the tested sample was placed in a temperature-controlled bath and a thermocouple inside the vessel was used to monitor the sample temperature.

## 3. Results and discussion

Corrugation and scrolling are intrinsic to the 2D graphene membrane [26]. Fig. 1 shows the corrugation clearly not only at the edge of the graphene but also in the middle of the nanosheets, and graphene nanosheets were folded and coiled. It is also highly possible that the folded or curved area will disappear and the sheet will become smooth in the fluid due to the absence of the external force to hold it. The size of graphene is in the range of  $0.2\text{--}2 \mu\text{m}$ . HRTEM image of the graphene illustrated the graphitic lattice clearly (Fig. 1d), and the interplanar distance was measured to be 0.43 nm, corresponding to the spacing of the (002) plane. The diffraction dots were indexed to the hexagonal graphite crystal structure. Most graphene nanosheets exist in style of thin few-layer graphene, and it was confirmed by noncontact mode atomic force microscopy (AFM). The cross-sectional view of the typical AFM image of the graphene (Fig. 1e, f) indicated that the thickness of graphene sheet was in the range of  $0.7\text{--}1.3 \text{ nm}$ .

Fourier transform infrared (FT-IR) spectroscopy and thermal analysis were conducted to confirm the formation of graphene. The graphene oxide showed the typical FT-IR absorption peaks at  $1726, 1630$  and  $1180 \text{ cm}^{-1}$ , corresponding to the vibration of C=O, O-H and C-O-C, respectively. While for the reduced graphene, almost all these peaks were invisible except the largely reduced vibration peak of C=O (Fig. 2a). There appears a new peak at  $1568 \text{ cm}^{-1}$ , which is attributed to the aromatic C=C group [27]. Graphene oxide was thermally unstable, and when it was heated, it would lose much weight, largely because of the elimination of absorbed water and the pyrolysis of the labile oxygen-containing functional groups. For the thermo-gravimetric (TG) analysis of the reduced graphene (Fig. 2b), it was found that reduced graphene displayed different thermal behaviors from that of graphene oxide. There was no obvious rapid decomposition process below  $430^\circ\text{C}$ , and the mass loss may be due to the absorbed water or gas molecules. Therefore the FT-IR and TG analysis provided solid evidence to explain that graphene oxide was reduced to graphene, and there are traces of unreduced oxygen-containing functional groups. It should be noted that surfactants (SDBS) used before the graphene oxide sheets are reduced are helpful in promoting stabilization. The possible stability mechanism is that: there is a weak non-covalent bond interaction between SDBS and graphene via  $\pi\text{--}\pi$  interactions [28]. During the reduction progress, the absorbed SDBS prevented the agglomeration of graphene. Due to the absorb interaction, SDBS cannot be removed completely during the rinse, and it is helpful in promoting the dispersion stability of graphene in polar solvents.

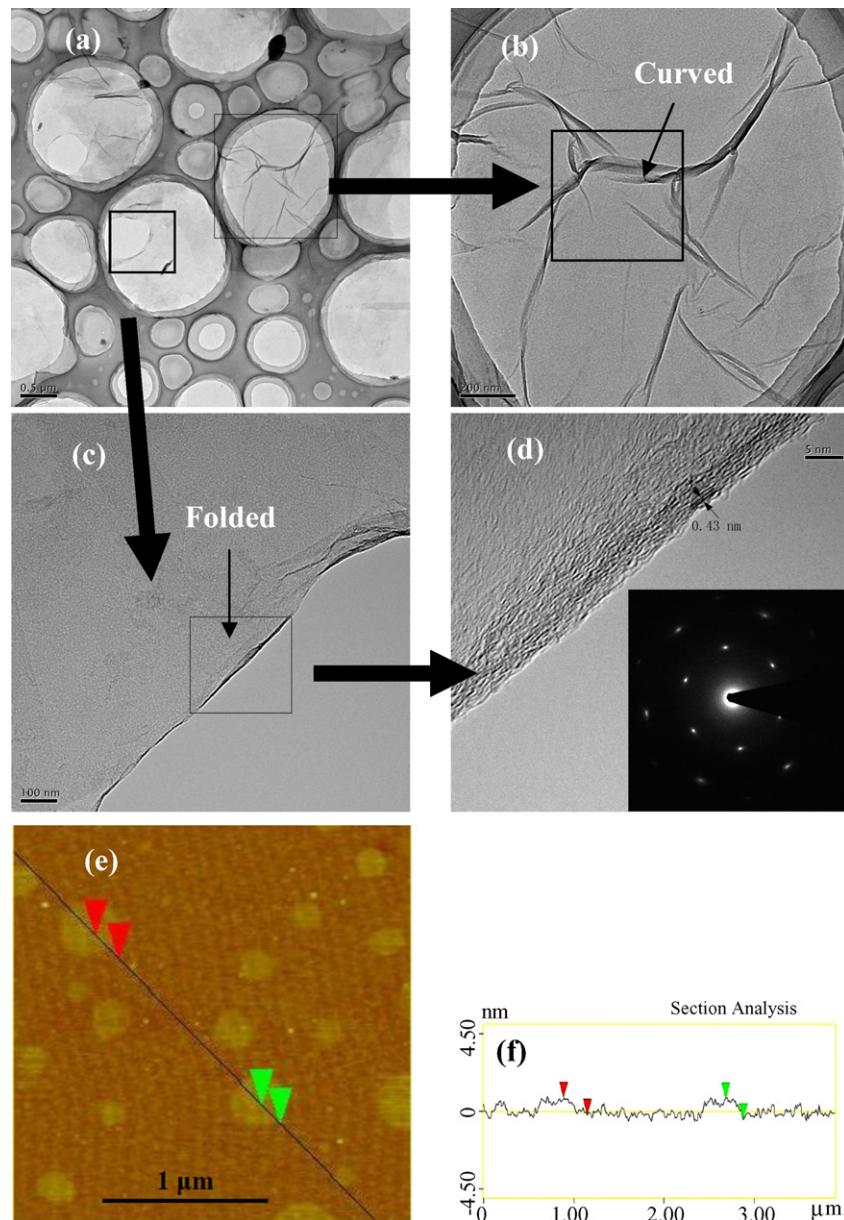


**Fig. 1.** TEM and AFM images of as-prepared graphene nanosheets. (a) bar 0.5  $\mu\text{m}$ ; (b) bar 200 nm, graphene wave in the middle; (c) bar 100 nm, graphene coiled at the edge; (d) HRTEM image of the graphene; (e) a tapping mode AFM image of graphene nanosheets, and (f) the height profiles in selected location.

Although nanofluids are used at various temperatures, thermal conductivity data for nanofluids as a function of temperature are lacking. Some groups have reported that there is a strong temperature dependence of thermal conductivity enhancement [29, 30], and they attributed the facts to the Brownian motion of the suspended nanoparticles and the micro-convection caused by the Brownian motions. However some researchers have reported the contrary results [31]. Therefore it is necessary to study the influence of temperature on the thermal conductivity enhancement of the nanofluids. Fig. 3a showed the thermal conductivity of 2.0 vol% and 5.0 vol% GN-EG nanofluids with the temperature range from 10 to 60  $^{\circ}\text{C}$ . The results illustrated that the temperature has little influence on the thermal conductivity enhancement, and the thermal conductivity of the nanofluids tracked that of the base fluid, and the enhancement ratios were almost constant in the tested temperature range, which was similar to the conclusion of Timofeeva [31] and Chen [32].

Fig. 3b depicted the thermal conductivity enhancement of GN-EG nanofluids as a function of loading at 30  $^{\circ}\text{C}$ . In the work,

$k$  and  $k_0$  represent the thermal conductivity of the nanofluid and base fluid, respectively, and  $(k - k_0)/k_0$  is the thermal conductivity enhancement ratio. For comparison, the thermal conductivity enhancement of GON-EG nanofluids was presented in Fig. 3b. It was seen that graphene was a good additive to enhance the thermal conductivity of the base fluid, and there was an approximate linear relationship between the enhancement ratio and volume fraction. When the loading was 5.0 vol%, the enhancement ratio was up to 86%, much larger than those containing metallic oxide and graphene oxide [23]. When graphene oxide was the additive with the volume fraction 5.0%, the enhancement ratio was 61%. Therefore the thermal conductivity enhancement ratio of GN-EG nanofluids was 1.42 times as that of GON-EG nanofluids.

Heat conduction mechanisms in nanofluids have been extensively scrutinized in the past decades to explain some experimental observations of their enhanced thermal conductivity. In the recent years, more and more evidences support the clustering mechanism. For example, Zhu et al. observed the clustering and alignment of  $\text{Fe}_3\text{O}_4$  nanoparticles, and they attributed the higher

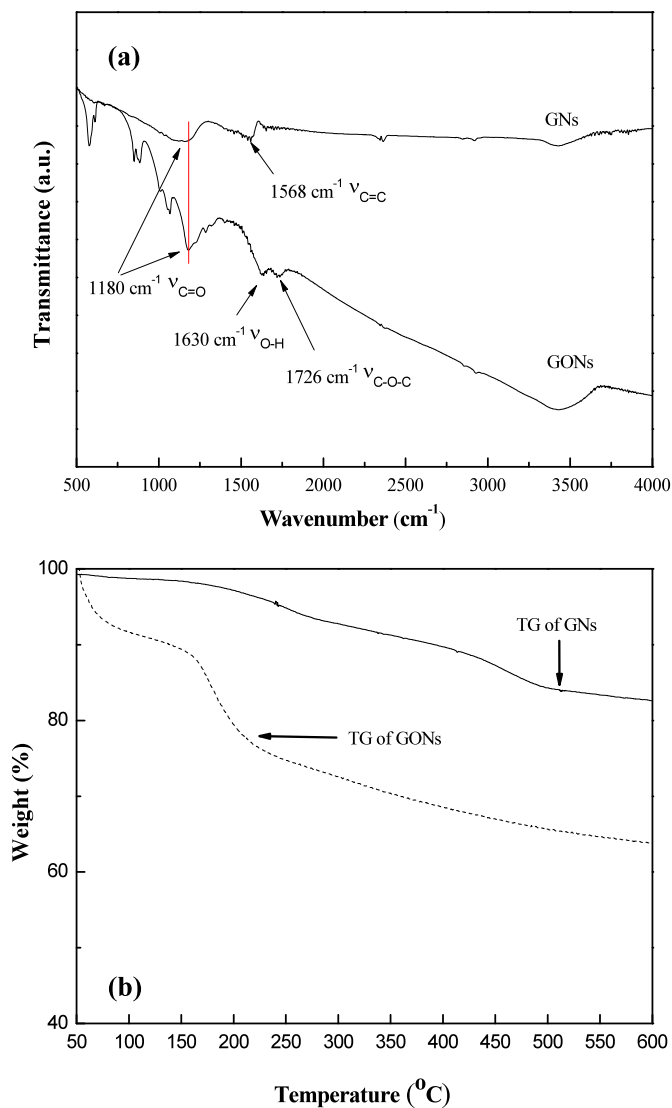


Fig. 2. The FT-IR and TG analysis of as-prepared graphene nanosheets (GNs) and graphene oxide nanosheets (GONs). (a) FT-IR spectra analysis; (b) TG analysis.

thermal conductivity of nanofluids to them [33]. The concepts of the thermal conductivity of aggregates and the effective volume fraction of aggregates were introduced into the Maxwell model to explain the experimental data [34]. Gao et al. [35] designed an experiment to explore the mechanism of thermal conductivity enhancement in nanofluids suggesting that clustering held the key for the thermal conductivity enhancement. Nanoparticles in the base fluids have the tendency to form clusters, and maybe clustering presents the major contributions to the high thermal conductivity of nanofluids. According to the prediction by Hamilton and Crosser [36], when the particle-to-liquid conductivity ratio of a suspension was above 100, the particle shape had a substantial effect on the effective thermal conductivity of the suspension. Gao et al. found that the adjustment of the nanoparticles shape was helpful to achieve appreciable enhancement of effective thermal conductivity [37]. Graphene itself is two-dimensional, and it has a very high aspect ratio and stiffness. These properties are helpful for the outstanding of thermal properties of GN-based nanofluids [15]. One unique feature of the GN-based nanofluids is that graphene has the largest surface area compared with nanotube and nanoparticle-based nanofluids due to the 2D structure of graphene. This means the graphene sheet will have significantly larger con-

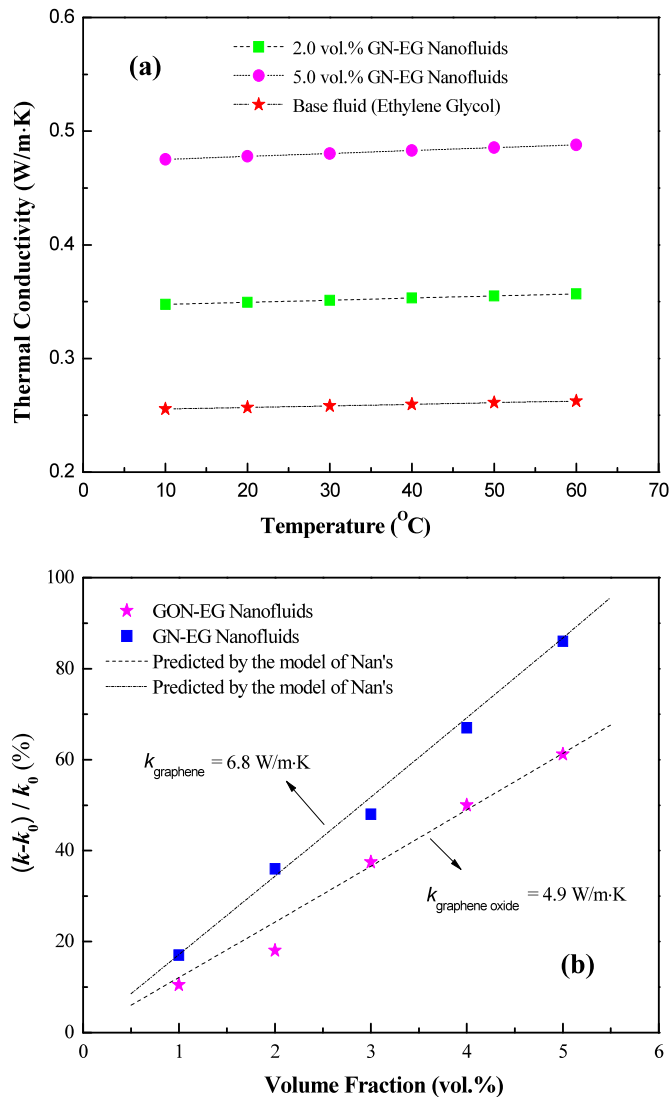


Fig. 3. The thermal conductivity and enhancement ratios of the nanofluids (a) the thermal conductivity of GN-EG nanofluids at different temperatures (the dash line is used to guide eyes); (b) the thermal conductivity enhancement ratios as a function of loading at 30 °C.

tact area/interface with the base fluid, therefore the contact resistance (Kapitza resistance) at the graphene–fluid interface will be reduced significantly. This will help improve the effective thermal conductivity of the nanofluid. With the same volume fraction, graphene sheets will extend more in space due to its 2D structure in comparison with nanoparticles and nanotubes. This large space extension will help transfer thermal energy. As a consequence, the thermal conductivity of the sheet itself plays an important role in thermal conductivity improvement. This partly explains why the GN-based nanofluid has a higher thermal conductivity increase than the nanofluids containing spherical nanoparticles.

Researchers from over 30 organizations worldwide completed a benchmark study on the thermal conductivity of nanofluids [38], and the results demonstrated that the experimental data were in good agreement with the effective medium theory developed for dispersed particles by Maxwell in 1881 and generalized by Nan et al. [39]. According to Nan's model, the resulting effective thermal conductivity of the composite for completely misoriented ellipsoidal particles is expressed as

$$k = k_0 \frac{3 + \varphi[2\beta_{11}(1 - L_{11}) + \beta_{33}(1 - L_{33})]}{3 - \varphi(2\beta_{11}L_{11} + \beta_{33}L_{33})}, \quad (1)$$

where  $L_{ii}$  and  $\phi$  are the geometrical factor and the volume fraction of particles, respectively.  $\beta_{ii}$  is defined as:

$$\beta_{ii} = \frac{k_p - k_0}{k_0 + L_{ii}(k_p - k_0)}, \quad (2)$$

where  $k_p$  is the thermal conductivity of the ellipsoidal particles. For graphene and graphene oxide, the aspect ratio is very high, so  $L_{11} = 0$  and  $L_{33} = 1$ . Based on Eq. (1) using least square fitting of the experiment data, we obtained the in-plane thermal conductivity of graphene oxide and graphene at  $4.9 \pm 0.6$  and  $6.8 \pm 0.8$  W/mK, respectively. It should be noted that the thermal conductivity calculated here by Nan's model has taken the matrix-additive interface contact resistance into consideration. In Eq. (1), the predicted thermal conductivity of composite is sensitive to the small change of thermal conductivity of the additive when it is 2D flake material. On the other hand, it is difficult to determine the thermal conductivity of nanoparticles from nanoparticle-based nanofluid thermal conductivity.

It was found that the thermal conductivity of graphene oxide and graphene estimated from the effective-medium approximation (Eq. (1)) is much lower than the intrinsic thermal conductivity of large-area graphene measured by Balandin et al. [7]. Graphene (or graphene oxide) prepared by the chemical method has a large size range from 0.2  $\mu\text{m}$  to 2  $\mu\text{m}$ , and the sizes of many graphene (or graphene oxide) nanosheets are much smaller than the phonon mean free path determined by the size of graphene. The thermal conductivity of graphene is limited by its size [40]. In addition, the thermal conductivity of chemically reduced graphene may be far below that of graphene due to the defects caused by the strong oxidization of graphite. The defects would never recover completely through the chemical or thermal reduction [41]. Our FT-IR analysis also confirmed that there were traces of unreduced oxygen-containing functional groups in the reduced graphene, although our reducing conditions were very rigorous. Schwamb et al. measured the thermal conductivity of reduced graphene oxide, and the samples exhibited a thermal conductivity only in the range of 0.14–2.87 W/mK [42]. The oxidized chemical structure introduced lattice defects which hinder thermal transport and promote diffusion effect. It should be noted that the property of graphene is influenced greatly by the preparing process, and its electrical conductivity is tunable in a large range [43]. Therefore the large thermal conductivity deviation among experiments by different groups is reasonable, and it strongly depends on the synthesis method. Second, theoretical calculation [10] demonstrated that the thermal conductivity of graphene depended strongly on the size of graphene, the edge roughness and concentration of defects. For the prepared reduced graphene, the nanosheets are always folded and coiled, which may influence the thermal conductivity greatly. The size of graphene prepared by this method was not large (in the range of 0.2–2  $\mu\text{m}$ ) due to the strong oxidation and ultrasonic exfoliation during the preparing process. Third, the trace of dispersant molecules adsorbed on the surface of graphene may significantly promote phonon scattering, and it has negative influence on the thermal conductivity of graphene. The GN-based nanofluids have better thermal transport than graphene oxide-based nanofluids. Graphene oxide consists of  $sp^2$ -hybridized carbon atoms and  $sp^3$ -hybridized carbons bearing hydroxyl and epoxide functional groups on either side of the sheet. The extensive presence of saturated  $sp^3$  bonds and oxygen atoms makes graphene oxide non-conducting, and hinders the thermal transport and promotes phonon scattering effects.

#### 4. Conclusions

In summary, we presented a simple method to prepare hydrophilic few-layer graphene, and the prepared graphene has good

compatibility with polar base fluids. The graphene sheet always exists in the state of corrugation and scrolling with its thickness in the range of 0.7–1.3 nm. The FT-IR and TG analysis confirmed that the graphene oxide was reduced to graphene. The GN-EG nanofluids showed substantial thermal conductivity increase over the base fluid. The temperature had little influence on the thermal conductivity enhancement. When the loading is 5.0 vol%, the enhancement ratio of thermal conductivity for GN-EG nanofluids was up to 86%, 42% higher than that of GON-EG nanofluids. The two-dimensional geometry, high aspect ratio and stiffness of graphene and graphene oxide are helpful to the outstanding thermal transport property of the pertaining nanofluids. The thermal conductivity of graphene oxide and graphene were estimated to be  $4.9 \pm 0.6$  and  $6.8 \pm 0.8$  W/mK, respectively. The size of graphene (or graphene oxide) used in this work is not very large, and many of them are much smaller than the phonon mean free path of graphene. This is one of the main reasons for the low thermal conductivity of the prepared graphene (or graphene oxide). In addition to the size of the graphene sheets, Kapitza resistance limits the measured thermal conductivity of graphene nanofluids. The extensive presence of saturated  $sp^3$  bonds and oxygen atoms makes graphene oxide non-conducting, and hinders the thermal transport and promotes phonon scattering. For the reduced graphene, the unsaturated and conjugated carbon atoms are restored, and it in turn improves electrical and thermal conductivity. On the other hand, defects in graphene caused by the strong oxidization of graphite, its small size and rough edge, and trace of dispersant molecules adsorbed on the graphene surface significantly promote phonon scattering and reduce its thermal conductivity.

#### Acknowledgements

The work was supported by Program for New Century Excellent Talents in University (NECT-10-883), Innovation Program of Shanghai Municipal Education Commission (10YZ199), and the Program for Professor of Special Appointment (Eastern Scholar) at Shanghai Institutions of Higher Learning. Partial support from NSF (CBET-0931290) is gratefully acknowledged.

#### References

- [1] A.K. Geim, K.S. Novoselov, *Nature Mater.* 6 (2007) 183.
- [2] K.S. Novoselov, A.K. Geim, S.V. Morozov, D. Jiang, Y. Zhang, S.V. Dubonos, I.V. Grigorieva, A.A. Firsov, *Science* 306 (2004) 666.
- [3] C. Berger, Z. Song, X. Li, X. Wu, N. Brown, C. Naud, D. Mayou, T. Li, J. Hass, A.N. Marchenkov, E.H. Conrad, P.N. First, W.A. de Heer, *Science* 312 (2006) 1191.
- [4] Z. Chen, Y.M. Lin, M.J. Rooks, P. Avouris, *Physica E* 40 (2007) 228.
- [5] F. Schedin, A.K. Geim, S.V. Morozov, E.W. Hill, P. Blake, M.I. Katsnelson, L.S. Novoselov, *Nature Mater.* 6 (2007) 652.
- [6] A.K. Geim, *Science* 324 (2009) 1530.
- [7] A.A. Balandin, S. Ghosh, W.Z. Bao, I. Calizo, D. Teweldebrhan, F. Miao, C.N. Lau, *Nano Lett.* 8 (2008) 902.
- [8] D.L. Nika, S. Ghosh, E.P. Pokatilov, A.A. Balandin, *Appl. Phys. Lett.* 20 (2009) 203103.
- [9] S. Ghosh, I. Calizo, D. Teweldebrhan, E.P. Pokatilov, D.L. Nika, A.A. Balandin, W. Bao, F. Miao, C.N. Lau, *Appl. Phys. Lett.* 92 (2008) 151911.
- [10] D.L. Nika, E.P. Pokatilov, A.S. Askerov, A.A. Balandin, *Phys. Rev. B* 79 (2009) 155413.
- [11] S. Ghosh, D.L. Nika, E.P. Pokatilov, A.A. Balandin, *New J. Phys.* 11 (2009) 095012.
- [12] Z. Guo, D. Zhang, X.G. Gong, *Appl. Phys. Lett.* 95 (2009) 163103.
- [13] J. Hu, X. Ruan, Y.P. Chen, *Nano Lett.* 9 (2009) 2730.
- [14] D. Konatham, A. Striolo, *Appl. Phys. Lett.* 95 (2009) 163105.
- [15] A.P. Yu, P. Ramesh, M.E. Itkis, E. Bekyarova, R.C. Haddon, *J. Phys. Chem. C* 111 (2007) 7565.
- [16] H.M. Duong, N. Yamamoto, K. Bui, D.V. Papavassiliou, S. Maruyama, B.L. Wardle, *J. Phys. Chem. C* 114 (2010) 8851.
- [17] H.M. Duong, N. Yamamoto, D.V. Papavassiliou, S. Maruyama, B.L. Wardle, *Nanotechnology* 20 (2009) 155702.
- [18] S. Park, R.S. Ruoff, *Nature Nanotech.* 4 (2009) 217.
- [19] S. Stankovich, R.D. Piner, X. Chen, N. Wu, S.T. Nguyen, R.S. Ruoff, *J. Mater. Chem.* 16 (2006) 155.

- [20] D. Li, M.B. Müller, S. Gilje, R.B. Kaner, G.G. Wallace, *Nature Nanotech.* 3 (2008) 101.
- [21] H.Q. Xie, H. Lee, W. Youn, M. Choi, *J. Appl. Phys.* 94 (2003) 4967.
- [22] J. Garg, B. Poudel, M. Chiesa, J.B. Gordon, J.J. Ma, J.B. Wang, Z.F. Ren, Y.T. Kang, H. Ohtani, J. Nanda, G.H. McKinley, G. Chen, *J. Appl. Phys.* 103 (2008) 074301.
- [23] W. Yu, H.Q. Xie, D. Bao, *Nanotechnology* 21 (2010) 055705.
- [24] Y.X. Xu, H. Bai, G.W. Lu, C. Li, G.Q. Shi, *J. Am. Chem. Soc.* 130 (2008) 5856.
- [25] G.X. Wang, B. Wang, J. Park, J. Yang, X.P. Shen, J. Yao, *Carbon* 47 (2009) 682009.
- [26] J.C. Meyer, A.K. Geim, M.I. Katsnelson, K.S. Novoselov, T.J. Booth, S. Roth, *Nature* 446 (2007) 60.
- [27] H.Q. Xie, H. Gu, M. Fujii, X. Zhang, *Meas. Sci. Technol.* 17 (2006) 208.
- [28] K.P. Loh, Q.L. Bao, P.K. Ang, J.X. Yang, *J. Mater. Chem.* 20 (2010) 2277.
- [29] C.H. Chon, K.D. Kihm, S.P. Lee, S.U.S. Choi, *Appl. Phys. Lett.* 87 (2005) 153107.
- [30] S.P. Jang, S.U.S. Choi, *Appl. Phys. Lett.* 84 (2004) 4316.
- [31] E.V. Timofeeva, A.N. Gavrilow, J.M. McCloskey, Y.V. Tolmachev, S. Sprunt, L.M. Lopatina, J.V. Selinger, *Phys. Rev. E* 76 (2007) 061203.
- [32] L.F. Chen, H.Q. Xie, L. Yang, W. Yu, *Thermochim. Acta* 477 (2008) 21.
- [33] H.T. Zhu, C.Y. Zhang, S. Liu, Y. Tang, Y. Yin, *Appl. Phys. Lett.* 89 (2006) 023123.
- [34] H.S. Chen, Y.L. Ding, C.Q. Tan, *New J. Phys.* 9 (2007) 367.
- [35] J.W. Gao, R.T. Zheng, H. Ohtani, D.S. Zhu, G. Chen, *Nano Lett.* 9 (2009) 4128.
- [36] R.L. Hamilton, O.K. Crosser, *Ind. Eng. Chem. Fundam.* 1 (1962) 187.
- [37] L. Gao, X.F. Zhou, *Phys. Lett. A* 348 (2006) 355.
- [38] J. Buongiorno, D.C. Venerus, N. Prabhat, T. McKrell, J. Townsend, R. Christianson, Y.V. Tolmachev, P. Keblinski, L.W. Hu, J.L. Alvarado, I.C. Bang, S.W. Bishnoi, M. Bonetti, F. Botz, A. Cecere, Y. Chang, G. Chen, H.S. Chen, S.J. Chung, M.K. Chyu, S.K. Das, R.D. Paola, Y.L. Ding, F. Dubois, G. Dzido, J. Eapen, W. Escher, D. Funfschilling, Q. Galand, J.W. Gao, P.E. Gharagozloo, K.E. Goodson, J.G. Gutierrez, H. Hong, M. Horton, K.S. Hwang, C.S. Iorio, S.P. Jang, A.B. Jarzebski, Y. Jiang, L. Jin, S. Kabelac, A. Kamath, M.A. Kedzierski, L.G. Kieng, C. Kim, J.H. Kim, S. Kim, S.H. Lee, K.C. Leong, I. Manna, B. Michel, R. Ni, H.E. Patel, J. Philip, D. Poulidakos, C. Reynaud, R. Savino, P.K. Singh, P. Song, T. Sundararajan, E. Timofeeva, T. Tritcak, A.N. Turanov, S.V. Vaerenbergh, D.S. Wen, S. Witharana, C. Yang, W.H. Yeh, X.Z. Zhao, S.Q. Zhou, *J. Appl. Phys.* 106 (2009) 094312.
- [39] C.W. Nan, R. Birringer, D.R. Clarke, H. Gleiter, *J. Appl. Phys.* 81 (1997) 6692.
- [40] S. Ghosh, W. Bao, D.L. Nika, S. Subrina, E.P. Pokatilov, C.N. Lau, A.A. Balandin, *Nature Mater.* 9 (2010) 555.
- [41] C. Gómez-Navarro, J.C. Meyer, R.S. Sundaram, A. Chuvilin, S. Kurasch, M. Burghard, K. Kern, U. Kaiser, *Nano Lett.* 10 (2010) 1144.
- [42] T. Schwamb, B.R. Burg, N.C. Schirmer, D. Poulidakos, *Nanotechnology* 20 (2009) 405704.
- [43] I. Jung, D.A. Dikin, R.D. Piner, R.S. Ruoff, *Nano Lett.* 8 (2008) 4283.